550.384.6

GLOBAL GEOMAGNETIC SECULAR VARIATION FROM 1956 TO 1976 AS DESCRIBED BY A FOUR-DIPOLE MODEL

by

H. NEVANLINNA
Department of Geophysics, University of Helsinki

and

Division of Geomagnetism, Finnish Meteorological Institute
Helsinki, Finland

Abstract

Secular variation data for alternate years between 1956 and 1976 from 43 geomagnetic observatories throughout the world were fitted into a four-dipole model giving an average rms error of 8.9 nT/y corresponding in accuracy to a 5th degree spherical harmonic analysis. The advantages of the dipole model seem to be its simplicity: 24 coefficients against the 35 coefficients of the corresponding spherical harmonic model, and perhaps more physical meaning although the dipoles do not coincide very well with the known regions of anomalous magnetic field.

The features of the isoporic field and the movements of isoporic foci obtained from charts based on the four-dipole model indicate that the rate of secular variation accelerated rapidly from 1956 to 1970, and has subsequently slowed down. The isoporic patterns have changed most in Eurasia, where the positive $\dot{Z}$ focus near the Caspian Sea disappeared in about 1960 and a negative focus formed in Southeast Asia and began drifting northeast. The areas of negative $\dot{Z}$ in the northern hemisphere and positive $\dot{Z}$ in the southern expanded during 1956–70. The intensification and expansion of the secular variation were seen in spherical harmonic coefficients, derived from the four-dipole model, as an acceleration in the decrease of the main axial dipole (g_1^0). By 1976 the acceleration of g_1^0 had ceased and the global isoporic field is now becoming more like that of the mid-fifties.

1. *Introduction*

The main geomagnetic field and its secular variation are usually described by spherical harmonic (SH) functions. Many attempts have been made to find more physical models than the SH models. These models use eccentric magnetic dipoles or circular current loops as sources of the geomagnetic field. ALLDREDGE and STEARNS [2], for example, used one geocentric and 34 eradial dipoles. ZIDAROV [41], ZIDAROV and BOCHEV [42] and BOCHEV [8] used models consisting of arbitrarily oriented dipoles. Recently ZIDAROV and PETROVA [43] and PEDDIE [33] studied models consisting of circular current loops.

In radial dipole models each eccentric dipole approximates an SH nondipole anomaly. The secular variation results from the drift and intensity changes of these dipoles.

Secular variation at a given epoch can also be represented directly by radial dipoles independent of the anomaly field. Each dipole corresponds then to a secular variation cell. LOWES and RUNCORN [25] modelled the global secular variation using 10 radial dipoles. Recently, NEVANLINNA [29] studied the secular variation in Europe using only one radial dipole corresponding to the well-known Caspian Z cell.

As shown by NEVANLINNA [30] and by NEVANLINNA and SUCKSDORFF [31], secular variation in Eurasia is described by two-dipole models as accurately as by SH models (n = 8) (BARRACLOUGH *et al.* [5, 6]) if the dipole parameters are determined using secular variation data only. Using the same principle, four radial and eccentric dipoles are used in this paper to model the global secular variation for alternate years from 1956 to 1976.

2. *Dipole model and parameters*

The magnetic field **B** at a point (θ,λ) on the Earth's surface caused by radial and eccentric dipole can be symbolised as follows:

$$\mathbf{B}(\theta,\lambda) = M\mathbf{F}(\theta,\lambda,\theta_0,\lambda_0,q_0) \tag{1}$$

where θ_0,λ_0,q_0 and M are the dipole parameters (P), (θ_0,λ_0) are the polar coordinates of the dipole (colatitude and east longitude), q_0, $0 \leqslant q_0 \leqslant 1$, is the radial distance from the geocentre divided by the Earth's radius (R_e), and M is the strength of the dipole in Teslas, that is $M = (\mu_0/4\pi)M_0R_e^{-3}$, where M_0 is the dipole moment (Am^2) and $\mu_0/4\pi = 10^{-7}\mathrm{Tm/A}$. The X, Y and Z components of the vector **F** are:

$$F_X = \cos\alpha(1 + 3q_0(\cos\beta - q_0)d^{-2})d^{-3}$$
$$F_Y = -F_X \cos\gamma/\cos\theta\cos\alpha \qquad (2)$$
$$F_Z = (\cos\beta - 3(\cos\beta - q_0)(1 - q_0\cos\beta)d^{-2})d^{-3}$$

where

$$\cos\alpha = \cos\theta \sin\theta_0 \cos(\lambda - \lambda_0) - \sin\theta \cos\theta_0$$
$$\cos\beta = \partial(\cos\alpha)/\partial\theta \qquad (2')$$
$$\cos\gamma = \partial(\cos\alpha)/\partial\lambda$$
$$d^2 = 1 + q_0^2 - 2q_0\cos\beta$$

The secular variation, $\dot{\mathbf{B}} = \partial\mathbf{B}/\partial t$, during a short time interval Δt can be calculated from Eq. (1) assuming linear changes in the parameters (P):

$$\dot{\mathbf{B}}(\theta,\lambda) = \frac{\partial(M\mathbf{F})}{\partial P}\dot{P} = M\left(\frac{\partial\mathbf{F}}{\partial\theta_0}\dot{\theta}_0 + \frac{\partial\mathbf{F}}{\partial\lambda_0}\dot{\lambda}_0 + \frac{\partial\mathbf{F}}{\partial q_0}\dot{q}_0\right) + \dot{M}\mathbf{F} \qquad (3)$$

The last term in the brackets can be ignored because the sources of the geomagnetic field are regarded as being located at a constant depth.

Usually the parameters P and their derivatives $\dot{P}$ are determined by the least-squares method using observed field values $\mathbf{B}$ and secular variation $\dot{\mathbf{B}}$. ALLDREDGE and STEARNS [2], for example, modelled the global geomagnetic field and its secular variation obtained from the IGRF for 1965 using 35 radial dipoles. The number of dipoles can be reduced if only secular variation data are used in the least-squares determinations of the dipole parameters and their changes.

In this paper a four-dipole model is used to describe the global secular variation during 1956–76. The secular variation was calculated from annual means taken from catalogues published by FISHER [15] and by PUSHKOV and IVCHENKO [36], see Table 1. In order to eliminate irregularities in the secular variation data, the annual means were first smoothed using three-year means. The yearly variation at the i'th observatory at the epoch t_0 is then given by

$$\dot{\mathbf{B}}_i(t_0) = \{\mathbf{B}_i(t_0 + 1.5) - \mathbf{B}_i(t_0 - 1.5)\}/3 \qquad (4)$$

The dipole parameters were calculated using the least-squares method, The square sum (S) was determined by

$$S = \sum_{i=1}^{N}\left\{\left\{\sum_{j=1}^{N'}\dot{\mathbf{B}}_j(\theta_i,\lambda_i,t_0)\right\} - \dot{\mathbf{B}}_i(t_0)\right\}^2, \qquad N = 43,\ N' = 4 \qquad (5)$$

Table 1. List of geomagnetic observatories used in the analysis.

Observatory	Code	Coordinates	
		θ	λ
Ebro	EBR	49.18°	0.49°E
Dombås	DOB	27.92	9.10
Fuerstenfeldbruck	FUR	41.83	11.28
Rude Skov	RSV	33.53	12.45
Lovö	LOV	30.66	17.82
Nurmijärvi	NUR	29.50	24.66
Sodankylä	SOD	22.64	26.63
Istanbul	ISK	48.94	29.06
Misallat	MLT	60.48	30.89
Moscow	MOS	34.53	37.32
Tbilisi	TFS	47.92	44.70
Vysokaya Dubrava	SVD	33.27	61.07
Tashkent	TKT	48.67	69.62
Kodaikanal	KOD	79.77	77.46
Dixon	DIK	16.45	80.57
Cape Chelyuskin	CCS	12.28	104.28
Irkutsk	IRT	37.83	104.45
Muntinlupa	MUT	75.62	121.02
Tixie	TIK	18.42	129.00
Yakutsk	YAK	27.98	129.72
Kakioka	KAK	53.77	140.62
Yuzhno-Sakhalinsk	YSS	43.05	142.72
Honolulu	HON	68.68	201.99
College	COL	25.14	212.16
Sitka	SIT	32.94	224.68
Meanook	MEA	35.38	246.67
Tucson	TUC	57.75	249.17
Fredericksburg	FRD	51.79	282.63
Ottawa	OTT	44.60	284.45
San Juan	SJG	71.89	293.85
Godhavn	GDH	20.76	306.48
San Miguel	SMG	52.23	334.35
Valentia	VAL	38.07	349.75
Lerwick	LER	29.87	358.82
Hermanus	HER	124.43	19.23
Tananarive	TAN	108.92	47.55
Gnangara	GNA	121.67	115.95
Toolangi	TOO	127.53	145.47
Amberley	AML	133.15	172.72
Apia	API	103.81	188.23
Huancayo	HUA	102.05	284.66
Pilar	PIL	121.67	296.12
Vassouras	VSS	112.40	316.35

where N is the number of observatories used and N' is the number of dipoles. The components of $\dot{\mathbf{B}}$ where $\dot{X}$, $\dot{Y}$ and $\dot{Z}$, so the square sum consisted of $3N$ (= 129) independent data points.

In Eq. (5), $\dot{\mathbf{B}}$ from Eq. (3) was written in the form:

$$\dot{\mathbf{B}}_j(\theta,\lambda) = c_{1j}(\partial \mathbf{F}/\partial\theta_0)_j + c_{2j}(\partial \mathbf{F}/\partial\lambda_0)_j + \dot{M}_j\mathbf{F}_j \tag{6}$$

where $c_{1j} = (M\dot{\theta}_0)_j$ and $c_{2j} = (M\dot{\lambda}_0)_j$. The first two terms in Eq. (6) describe the secular variation caused by the drift of a dipole, and the last term the secular variation caused by changes in the dipole moment. Because only secular variation data are used in Eq. (5), the strength M_j and the drift rates $(\dot{\theta}_0,\dot{\lambda}_0)_j$ cannot be completely separated from each other, and only their products c_{1j} and c_{2j} can be determined. There were thus 24 coefficients $(\theta_0,\lambda_0,q_0,c_1,c_2,\dot{M})_j$, j = 1,..., 4 to be determined by the least-squares method.

The dipole parameters were calculated using a computer program system called MINUIT (JAMES and ROOS [20]). MINUIT is specially designed to minimize nonlinear functions like S in Eq. (5). Only 15 parameters at a time can be determined by MINUIT. During one iteration 5 parameters thus had to be kept fixed; during next run these were free and 5 others fixed. This iteration procedure was continued until the nms error $(\sqrt{S/3N})$ did not change by more than 0.05nT/y.

The parameters were determined in two stages: first, the dipoles were fixed to correspond to four SH nondipole anomalies: the Asian, African, North American and Australian Z anomalies, which, according to YUKUTAKE and TACHINAKA [39], are the most rapidly changing anomalies of continental size. Table 2 shows the parameters $(\theta_0,\lambda_0,M)_j$. $(\theta_0,\lambda_0)_j$ is the focal point of SH nondipole Z taken from charts published by YUKUTAKE and TACHINAKA [39] for the epoch 1965.0. The strength M_j was calculated from chart values of nondipole Z as follows:

$$M = -0.5(1 - q_0)^3 Z_f \tag{7}$$

Table 2. Data for SH nondipole anomalies for 1965.0 based on chart values by YUKUTAKE and TACHINAKA [39].

	Asia	Africa	North America	Australia
θ_0	45°	90	45	135
λ_0	105°E	0	270	135
Z_f	18000nT	−16000	6500	−12000
M	−3800nT	3400	−1370	2530

where Z_f is the focal value of nondipole Z. q_0 was fixed at 0.25 in order to get the same mean great circle distance (c. 70°) as in the SH nondipole charts between $+X_f$ and $-X_f$ (or $+Y_f$ and $-Y_f$) around the Z focus. The value $q_0 = 0.25$ is also the mean value of q_0 in the dipole models by ALLDREDGE and HURWITZ [1], ALLDREDGE and STEARNS [2] and NEVANLINNA [30].

Since the position and strength of the dipoles were fixed, the derivatives $\dot{P}$ were determined by the least-squares method using Eq. (5). In this first stage, 12 parameters were thus determined. The model obtained in the first stage is in principle similar to the models *e.g.* by ALLDREDGE and STEARNS [2]: the four-dipole model here describes the anomaly field via the parameters P and the secular variation caused by the changes in the anomaly field, via the derivatives $\dot{P}$. However, the rms error between model and observed secular variation was rather high, 18 – 20nT/y, though the global features of isoporic lines and the positions of isoporic cells were essentially the same as in SH maps for the corresponding epochs.

The reason for the high rms error is probably in the inaccurate description of the anomaly field by the four dipoles. Especially important are the gradient terms $\partial \mathbf{F}/\partial\theta_0$ and $\partial \mathbf{F}/\partial\lambda_0$, because small errors in field gradients cause large errors in the drifting part of secular variation.

One possible way of obtaining better description of the secular variation is to improve the description of the anomaly field by adding more dipoles to the model, as was done by ALLDREDGE and STEARNS [2]. The second method used here is to free the dipole locations $(\theta_0,\lambda_0)_j$. Thus all the dipole parameters and their changes are determined only from secular variation data. This is a crucial step because the locations of the dipoles are no longer constrained by the anomaly field and thus the dipoles do not describe the observed anomaly field. Because the dipoles are now free, the gradients $\partial \mathbf{F}/\partial\theta_0$ and $\partial \mathbf{F}/\partial\lambda_0$ will now be optimized. Thus the secular variation is described more accurately than in the first stage. The final rms errors were reduced by roughly 50 %: the mean vector rms error for 11 epochs between 1956 and 1976 was 8.9nT/y.

The parameters giving the lowest rms error are shown in Table 3. As can be seen in this table and in Figs. 1, 2 and 3, the dipoles have a clear tendency to locate near the dominant $\dot{Z}$ cells in Central Asia, Atlantic Ocean and Antarctic. Thus the secular variation in Asia and East Europe is mainly described by the changes in the dipole j = 1. The secular variation over an area from North and South America and Western Europe is described mainly by the changes in the dipoles j = 2 and 3, which are located close to each other. The secular variation in the Indian Ocean and Australia is represented mainly by the changes in the dipole j = 4.

Table 3. Coefficients of four-dipole models for 1956–1976. θ_0 and λ_0 are given in degrees of arc, c_1 and c_2 in nTdeg/y and $\dot{M}$ in nT/y. All the dipoles are located at a radial distance of $0.25\,R_e$ from the geocentre.

dipole	epoch	1956.0	1958.0	1960.0	1962.0	1964.0	1966.0	1968.0	1970.0	1972.0	1974.0	1976.0
j=1	θ_0	76.6	70.8	35.8	35.6	40.2	18.6	18.9	19.3	39.6	23.1	35.3
	λ_0	59.0	64.4	122.0	130.8	156.5	116.2	97.8	83.1	118.5	135.0	77.7
	c_1	400.4	222.7	225.3	248.7	−32.7	265.8	208.5	226.1	−246.2	−148.2	−409.9
	c_2	311.4	294.5	374.9	212.0	−172.9	45.4	315.1	599.0	−48.4	60.6	86.2
	$\dot{M}$	0.75	0.27	4.78	5.23	7.64	5.40	7.50	8.37	10.85	15.80	7.97
j = 2	θ_0	93.7	94.5	91.8	83.9	89.8	83.1	90.5	74.6	85.4	83.0	83.3
	λ_0	−61.7	−62.0	−62.5	−66.0	−64.1	−67.6	−65.4	−73.6	−61.6	−64.6	−64.1
	c_1	−800.4	−765.3	−621.2	−930.2	−691.9	−603.2	−904.4	−1089.4	−578.0	−397.1	−668.8
	c_2	1196.5	−1138.0	1250.2	2029.5	1326.0	1589.5	1139.0	2797.9	1262.1	1025.1	1224.7
	$\dot{M}$	25.54	22.84	19.76	21.39	23.63	25.84	30.43	23.89	23.08	21.61	18.4
j = 3	θ_0	49.4	45.3	49.1	58.3	39.2	49.2	38.3	54.4	40.4	34.6	35.6
	λ_0	271.8	270.7	277.0	283.7	270.4	277.2	273.7	277.8	288.2	283.4	289.6
	c_1	205.6	269.5	442.4	779.3	542.5	553.9	324.6	1416.6	888.7	994.5	956.8
	c_2	−865.0	−836.9	−834.6	−1459.1	−933.9	−1210.1	−1069.1	−2285.2	−1007.5	−732.7	−1079.9
	$\dot{M}$	−5.92	−6.49	−0.76	−2.94	−4.69	−3.55	−13.85	−5.96	−11.12	−11.95	−12.29
j = 4	θ_0	152.0	154.6	146.2	134.5	130.7	150.5	153.0	148.6	143.9	150.9	147.0
	λ_0	69.3	72.1	72.0	51.0	57.4	71.8	71.8	71.4	76.3	90.3	87.3
	c_1	−145.2	−204.2	−457.2	−316.8	−503.0	−411.6	−174.6	−185.9	−434.1	−567.5	−701.6
	c_2	1247.3	1265.0	989.2	809.6	867.3	1123.1	1163.8	880.4	1019.1	1188.8	1241.2
	$\dot{M}$	−11.80	−11.73	−9.16	−10.41	−8.49	−13.72	−15.18	−12.22	−17.93	−13.68	−14.63

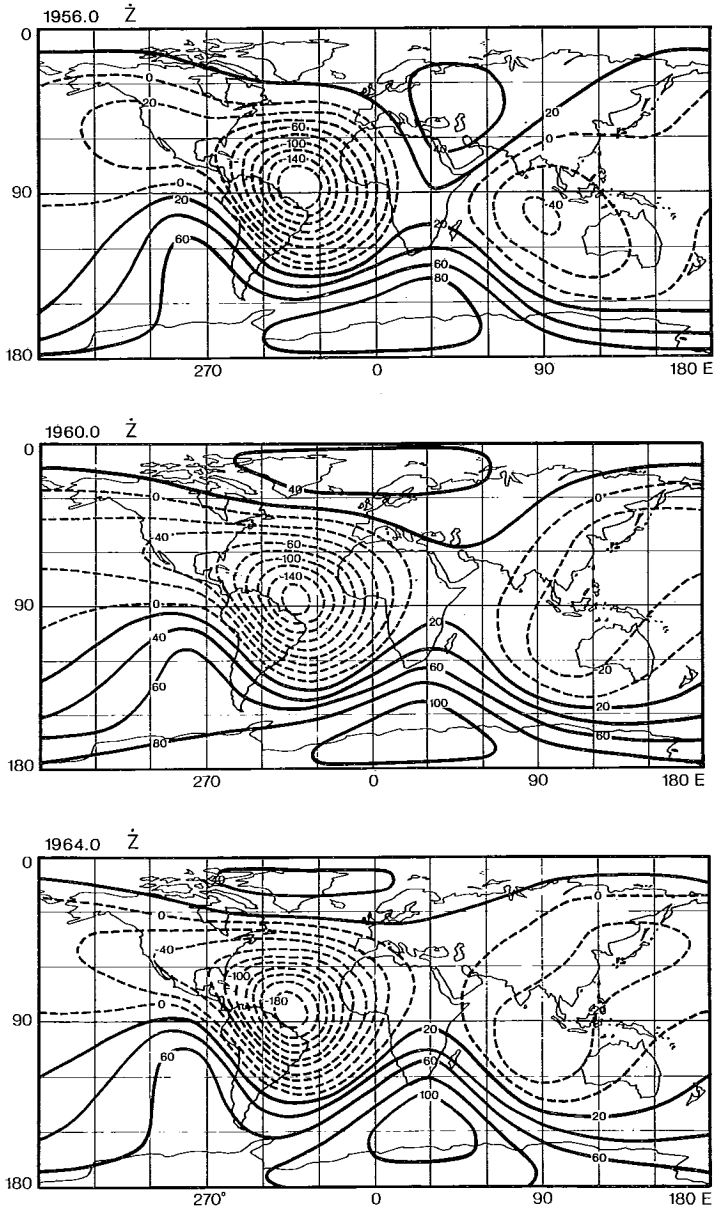

Fig. 1. The yearly secular variation of Z (with a contour interval of 20nT/y) for the epochs 1956.0, 1960.0, and 1964.0 as calculated from the four-dipole model in Table 3.
Solid lines: $\dot{Z} > 0$.
Dotted lines: $\dot{Z} \leqslant 0$.

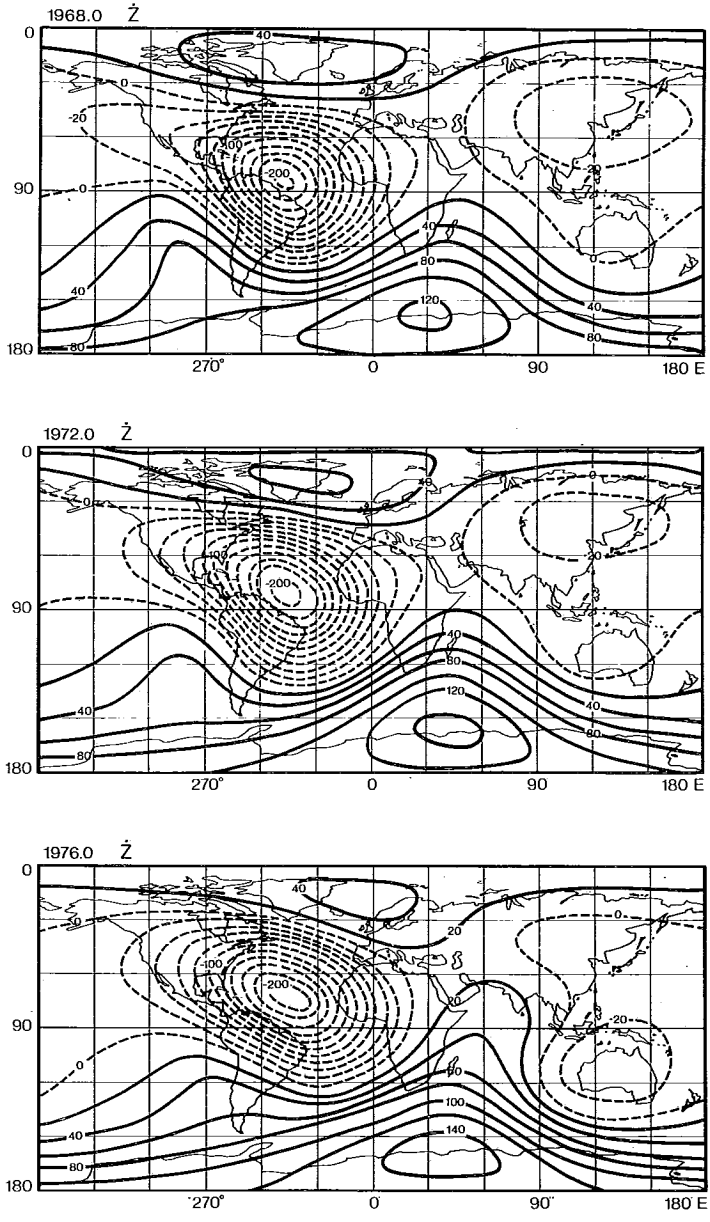

Fig. 2. The yearly secular variation of Z (with a contour interval of 20nT/y) for the epochs 1968.0, 1972.0 and 1976.0 as calculated from the four-dipole model in Table 3.
Solid lines: $\dot{Z} > 0$.
Dotted lines: $\dot{Z} \leqslant 0$.

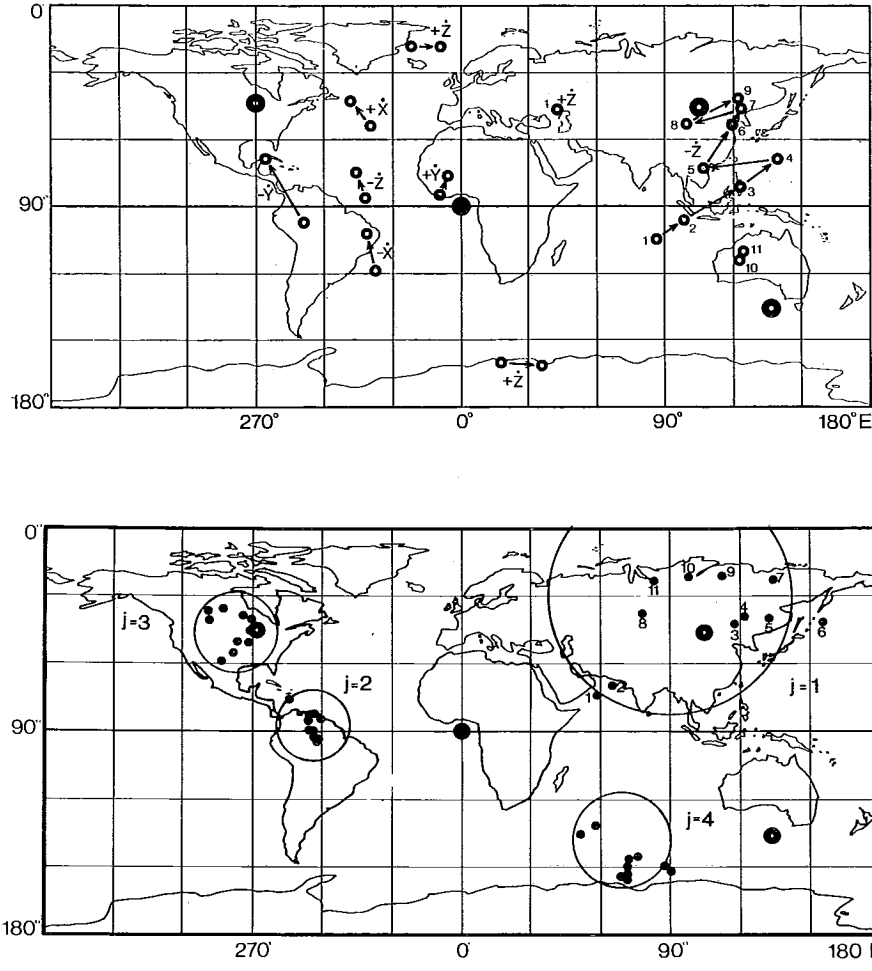

Fig. 3. Top: Locations (small circles) of $\dot{X}$, $\dot{Y}$ and $\dot{Z}$ isoporic foci from maps based on the four-dipole model in Table 3. The arrows give the total drift of the foci from 1956 to 1976 except in Asia and Australia where $\dot{Z}$ foci are numbered 1, 2,..., 11 corresponding to the epochs 1956.0, 1958.0,..., 1976.0. Large circles denote the foci of the SH nondipole anomalies from Table 2.

Below: The locations $(\theta_0, \lambda_0)_j$ of the dipoles for alternate years between 1956 and 1976 according to Table 3. The locations in Asia are numbered in the same way as the corresponding $\dot{Z}$ foci. The circle around the dipole locations is the circle of 95 % confidence.

As can be seen further in Table 3 and Fig. 3, the locations $(\theta_0,\lambda_0)_j$ of the dipoles j = 2, 3 and 4 from one epoch to another are distributed over a rather small area: the scatter, as measured by the radius of the 95 % confidence circle (α_{95}), is about 15° for these dipoles. On the other hand, the dipole j = 1 describing the secular variation in Asia and Eastern Europe, has moved within 100° in longitude and 20° in latitude (α_{95} = 52°).

The coefficients c_1 and c_2 in Table 3 describing the secular variation caused by drift of the anomaly field are clearly greater for the dipoles j = 2, 3 and 4 than for the dipole j = 1. This means that intensity changes, described by the term $\dot{M}\mathbf{F}$ in Eq. (6), dominate the secular variation in Asia and Eastern Europe. As can be seen in Eqs. (1) and (6) the term $\dot{M}\mathbf{F}$ can be interpreted as a radial dipole under the focus of a $\dot{Z}$ cell. If the cell is moving, the corresponding dipole follows it. Figs. 1, 2 and 3 show that the movements of $\dot{Z}$ foci and the locations $(\theta_0,\lambda_0)_1$ of the dipole over Asia have been similar. The rapid movement, up to 20°/y, of $\dot{Z}$ focus in Asia, is probably not caused by corresponding movements of the core fluid which is known to cause a westward drift of only 0.2–0.3°/y. The apparent movement observed can be explained by intensification and consequently a northward expansion of the equatorial negative $\dot{Z}$ zone.

The locations of the other dipoles are determined partly by the term $\dot{M}\mathbf{F}$ and partly by the gradient terms describing the drifting part of the field. The tendency of the dipoles to locate under the $\dot{Z}$ foci due to the term $\dot{M}\mathbf{F}$ is opposed by the gradient terms which force the dipoles to locate 30–50° away from the $\dot{Z}$ foci so that the gradients of the Z field are at their maximum at the $\dot{Z}$ foci.

2.1 Four-dipole model compared with SH model

To estimate the harmonic degree (n) of an SH model of the secular variation corresponding in accuracy to the four-dipole model, the dipole parameters were calculated using exactly the same data set as used by MALIN and CLARK [27] for their calculation of an SH model of degree n = 6. This data set consists of annual means for the epochs 1962.5 and 1967.5 from 118 geomagnetic observatories throughout the world. The yearly secular variation is thus a 5-year mean centred at 1965.0. The comparison is shown in Fig. 4, which depicts the vector rms errors for the secular variation as functions of n, and of the number (n_d) of coefficients in the models. As can be seen, the four-dipole model after the first stage (n_d = 12) gives an rms error of 18nT/y. The same error is obtained in the SH model with n between 2 and 3. After the second stage (n_d = 20) the rms error is 10.0nT/y, corresponding to a harmonic degree n = 5. When q_0's were also free (n_d = 24) the

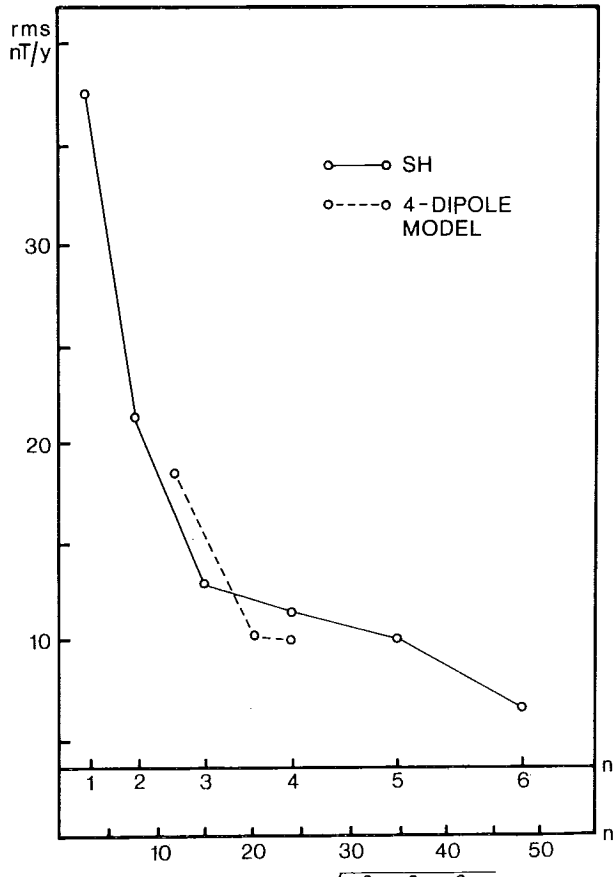

Fig. 4. Comparison of vectors rms errors ($\sigma = \sqrt{(\sigma_X^2 + \sigma_Y^2 + \sigma_Z^2)/3}$) of four-dipole model of annual secular variation from 118 geomagnetic observatories at the epoch 1965.0. The data used have published by MALIN and CLARK [27]. n is the harmonic degree and n_d the number of coefficients in both models.

rms error improved by only 0.1 nT/y. Thus the number of coefficients in the four-dipole model is about 60 % of that in the corresponding 5th degree SH model with 35 coefficients.

The gaussian coefficients ($\dot{g}_n^m, \dot{h}_n^m$) of an SH model equivalent to the four-dipole model, can be calculated by solving the Laplace equation for the magnetic potential (V) of an eccentric dipole using SH functions. For one dipole, the potential can be written as follows (see HURWITZ [17]:

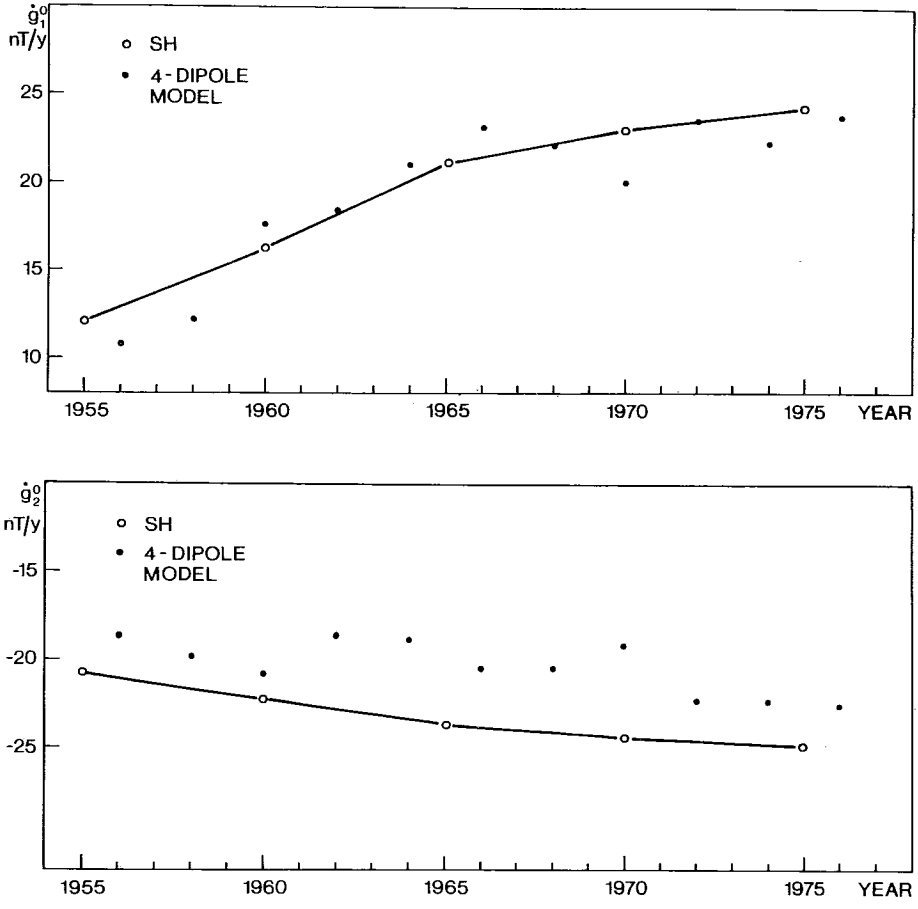

Fig. 5. $\dot{g}_1^0$ and $\dot{g}_2^0$ (solid circles) as calculated from the four-dipole models in Table 3. The open circles denote $\dot{g}_1^0$ and $\dot{g}_2^0$ obtained from SH models by MALIN [27] for 1965.0, HURWITZ *et al.* [19] for 1970.0 and by PEDDIE and FABIANO [34] for 1975.0.

$$V = R_e \sum_{n=1}^{\infty} \sum_{m=0}^{n} (A_n^m \cos m\lambda + B_n^m \sin m\lambda) P_n^m(\cos\theta) \tag{8}$$

where

$$A_n^m = M q_0^{n-1} n P_n^m(\cos\theta_0)\cos m\lambda_0 \,, \qquad B_n^n = A_n^m \tan m\lambda_0 \tag{8'}$$

where $P_n^m(\cos\theta)$ is Schmidt's quasi-normalized associated Legendre function (CHAPMAN and BARTELS [11]). The Gaussian coefficients are thus

$$g_n^m = A_n^m \,, \quad h_n^m = A_n^m \tan m\lambda_0 \tag{9}$$

For a secular variation model consisting of N' radial dipoles at q_0, we get from Eqs. (8') and (9)

$$\begin{aligned}\dot{g}_n^m &= \sum_{j=1}^{N'} nq_0^{n-1}\{\dot{M}_j P_n^m(\cos\theta_{0j})\cos m\lambda_{0j} + c_{1j}(\partial P_n^m(\cos\theta)/\partial\theta)_{\theta=\theta_{0j}}\cos m\lambda_{0j} \\ &\quad - c_{2j} m P_n^m(\cos\theta_{0j})\sin m\lambda_{0j}\} \\ \dot{h}_n^m &= \sum_{j=1}^{N'} (\{(\dot{g}_n^m)_j \sin m\lambda_{0j} + c_{2j} q_0^{n-1} mn P_n^m(\cos\theta_{0j})\}/\cos m\lambda_{0j})\end{aligned} \tag{10}$$

As examples, the axial dipole and quadrupole terms $\dot{g}_1^0$ and $\dot{g}_2^0$ calculated from Eqs. (9) and (10) for 11 epochs are shown in Fig. 5 together with corresponding terms obtained from direct SH analysis. The rather good correlation between $\dot{g}_1^0$ calculated from four-dipole and SH models indicates that, as in the models by ALLDREDGE and STEARNS [2], a separate geocentric dipole is not needed in the dipole models because the contribution of the geocentric dipole is included in the eccentric dipoles.

3. *Global features of the isoporic field*

3.1 Isoporic foci

Because the four-dipole models shown in Table 3 describe the global secular variation with reasonable accuracy, they can be used to study the typical features of the global isoporic lines at different epochs from 1956 to 1976.

The charts in Figs. 1 and 2, calculated from the dipole parameters in Table 3 and depicting the isopores of $\dot{Z}$, are of special interest because $\dot{Z}$ foci reveal the locations where changes in the magnetic flux enter from the core to the mantle. The locations and intensities of the $\dot{Z}$ foci, as well as those of $\dot{X}$ and $\dot{Y}$ shown in Fig. 3, are consistent with the corresponding values obtained from SH models by LEATON [23], MALIN [26], MALIN and CLARK [27] and DAWSON and NEWITT [13], which cover the same time interval as studied here. On a global basis, there are the following isoporic foci (see also Fig. 3). In $\dot{X}$, two well-defined foci are located in the Atlantic, a positive (c. 90nT/y at 1976) at (45°N, 310°E) and a negative (c. −110nT/y) at (15°S, 320°E). In $\dot{Y}$ there is a negative focus (c. −60nT/y) in Central America at (20°N, 270°E) and a positive (c. 80nT/y) in West Africa at (15°N, 350°E). In $\dot{Z}$ there is a dominant negative focus (c. −220nT/y) in the mid-Atlantic at (15°N, 315°E). As can be seen from Fig. 3 these foci have drifted about 10° northwest from 1956 to 1976. Thus in the near future the secular variation

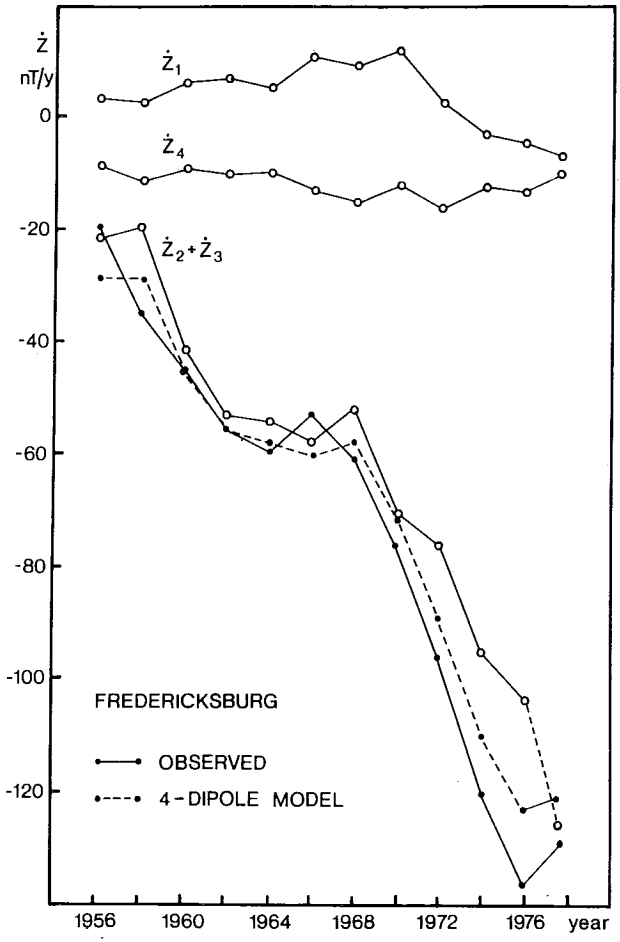

Fig. 6. The observed secular variation of Z (line with solid circles) at the Fredericksburg observatory, USA. The dotted curve depicts $\dot{Z}$ as calculated from the four-dipole model in Table 3. The curve denoted by $\dot{Z}_2 + \dot{Z}_3$ represents the contribution of dipoles j = 2 and 3 describing the Atlantic $\dot{Z}$ cell. The curves denoted by $\dot{Z}_1$ and $\dot{Z}_4$ represent the contribution from the dipoles j = 1 and 4.

will accelerate in the North American continent. As was pointed out by DAWSON and NEWITT [13], LANGEL *et al.* [22] and CAIN [9], $\dot{Z}$ has rapidly decreased in the eastern USA. This can be seen in Fig. 6, which depicts the secular variation of Z at the Fredericksburg observatory (see Table 1) in the eastern USA. In twenty years $\dot{Z}$ has dropped there from −20nT/y to −14nT/y.

In $\dot{Z}$ there are also two positive foci, a weaker (c. 40nT/y) near Iceland at

(75°N, 350°E) and a stronger (c. 140nT/y) in the Antarctic at (65°S, 40°E). These have drifted about 15° eastwards during the time interval studied.

In Asia, at the epoch 1956, there was a positive $\dot{Z}$ focus (c. 40nT/y) near the Caspian Sea at (45°N, 45°E). This cell was the dominant source of secular variation in Europe and west Asia, at least from 1840 to 1950 (NEVANLINNA [29]). Its intensity was highest (c. 130nT/y) in about 1910, as can be seen from SH maps, *e.g.* those of CAIN and HENDRICKS [10], after which the intensity weakened steadily and the focus disappeared completely in about 1960. This remarkable disappearance has also been reported by ORLOV [32], TAZIMA *et al.* [37] and POCHTAREV [35]. At this time, the negative focus (c. −40nT/y) in the Indian Ocean (15°S, 90°E) was moving northeast and forming a negative focus (c. −30 nT/y) near the focus of the Asian SH nondipole anomaly at (45°N, 105°E) in agreement with SH maps prepared by DOLGINOV *et al.* [14]. This focus disappeared in about 1972 and a new negative focus was formed in eastern Australia near the 1956 location of the negative focus.

In Asia, the secular variation of Z is now developing towards positive $\dot{Z}$ values and a new positive $\dot{Z}$ focus is forming from the bulge of the isoporic lines near India, as can be seen in the $\dot{Z}$ chart for 1976.0 in Fig. 2. Thus the secular variation of Z in Asia and eastern Europe has been cyclic with a period of about 20 years.

3.2 Drift of $\dot{X}$ and $\dot{Y}$ isopores

As demonstrated in the previous chapter, the patterns of isoporic lines have changed most in Eurasia and Australia. These changes can be seen in an interesting way in the oscillating drifts of the $\dot{X}$ and $\dot{Y}$ isolines.

In 1956, the zero $\dot{X}$ line in Eurasia was flowing roughly in the east-west direction (see Fig. 7) at about 45°N. $\dot{X}$ was positive south of this line. Until 1970 the zero line was moving to the northeast, up to 75°N, after which it drifted back to the southeast. In 1976 the zero line of $\dot{X}$ was about 70°N.

In 1956, Eurasia was divided into two blocks by zero $\dot{Y}$ lines. $\dot{Y}$ was positive west of the zero line, which lay in the north-south direction at about 50°E. East of this line $\dot{Y}$ was negative through Asia except for the southeast corner of the continent. The western zero line drifted westwards up to 1970. In 1970 this line was flowing in the northwest direction from Iceland to Central Europe and the Near East (see Fig. 7). The eastern zero line first moved up to 145°E to the southeast and then rapidly to the west reaching about 100°E. During 1970–76 both the western and eastern zero lines drifted eastwards towards the position they had occupied in 1956.

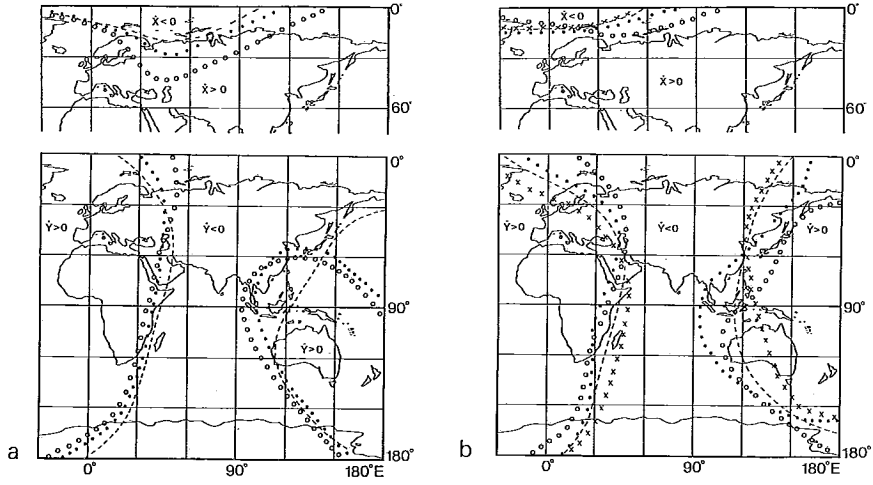

Fig. 7. Zero lines of $\dot{X}$ and $\dot{Y}$ obtained from isoporic charts based on the four-dipole model in Table 3.

a. Top: Zero lines of $\dot{X}$
Below: Zero lines of $\dot{Y}$
o 1956.0
• 1958.0
– 1960.0

b. Top: Zero lines of $\dot{X}$
Below: Zero lines of $\dot{Y}$
o 1962.0
• 1964.0
– 1966.0
x 1968.0

c. Top: Zero lines of $\dot{X}$
Below: Zero lines of $\dot{Y}$
o 1970.0
• 1972.0
– 1974.0
x 1976.0

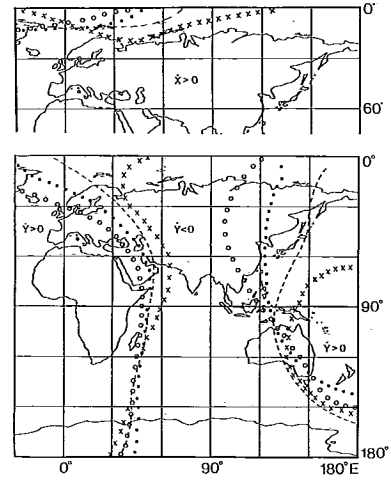

As can be seen from Fig. 7, the zero lines of $\dot{Y}$ have also drifted in the southern hemisphere, but with much smaller amplitude and in the opposite direction to the drift in the northern hemisphere.

As an example from northern Europe, where the oscillation of $\dot{Y}$ has been most intense, the $\dot{Y}$ curve from Nurmijärvi (Finland) is shown in Fig. 9. This clearly shows that the oscillating part of $\dot{Y}$ is caused by the dipole describing the secular

variation in Asia, since the contributions from other dipoles are roughly linear.

These rapid changes in $\dot{Y}$ have perhaps been one reason for the inaccuracy of the secular variation of IGRF of 1965.0 in Scandinavia. As reported by BARRACLOUGH [3, 4], SH $\dot{Y}$ in Scandinavia was about 13 nT/y higher on average than the observatory values. Because IGRF is based mainly on the pre-1965 values and has only linear secular variation terms, it was unable to predict the rapid decrease of $\dot{Y}$ around 1965. In a later SH model (n = 8) for 1967.5 by HURWITZ *et al.* [18], the rms error for five Scandinavian observatories was 5 nT/y, indicating that the secular variation is not anomalous in Scandinavia but that the poor fit of $\dot{Y}$ in IGRF is due to inaccurate prediction of the secular variation.

$\dot{X}$ is now changing in the same way as $\dot{Y}$ did around 1965. The zero line of $\dot{X}$ is drifting rapidly to the southwest in Europe. In 1975 $\dot{X}$ was zero at Ny-Aalesund (78.9°N, 11.9°E) (BERGER and BREKKE [7]) and in 1977 at Nurmijärvi. In 1980 the zero line of $\dot{X}$ will probably cross Central Europe. Thus, as pointed out by BARRACLOUGH *et al.* [5, 6], the IGRF for 1980 should include some secular acceleration terms in order to better consider the very recent trends in the secular variation, for example the rapid decrease of $\dot{X}$ in Europe.

3.3 Foci of horizontal vectors of secular variation

As demonstrated in the previous chapters by movements of $\dot{Z}$ foci and by drifts of $\dot{X}$ and $\dot{Y}$ zero isopores, the secular variation in Eurasia has been cyclic with a period of about 20 years. This cyclic secular variation was studied, independent of the four-dipole model, using Fourier-series representation of annual means from 40 geomagnetic observatories from 1953 to 1975 (see Fig. 8).

To obtain the Fourier coefficients for each observatory, a linear part, determined by the straight line going through the first and last data point, was first subtracted from the annual means and the mean value of the residuals was then adjusted zero. A Fourier series with $T = 22$ year as the fundamental period and wave numbers (k) from 1 to 10, was the fitted to these residuals. The secular variation of X and Y was then obtained by differentiating the series with respect to time t:

$$(\dot{X}, \dot{Y}) = \sum_{k=1}^{\ell} (k\omega\{-(a_{\dot{X}}, a_{\dot{Y}})_k \sin(k\omega t) + (b_{\dot{X}}, b_{\dot{Y}})_k \cos(k\omega t)\}) \qquad (11)$$

$$\omega = 2\pi/T\,, \qquad \ell = 10\,, \qquad T = 22\,\mathrm{y}$$

Fig. 8 shows the distribution of $(\dot{X}, \dot{Y})$ vectors when $T = 22$ y, and the vector sum for $T = 11$ y and the constant part of the horizontal secular variation, all for epoch 1972.

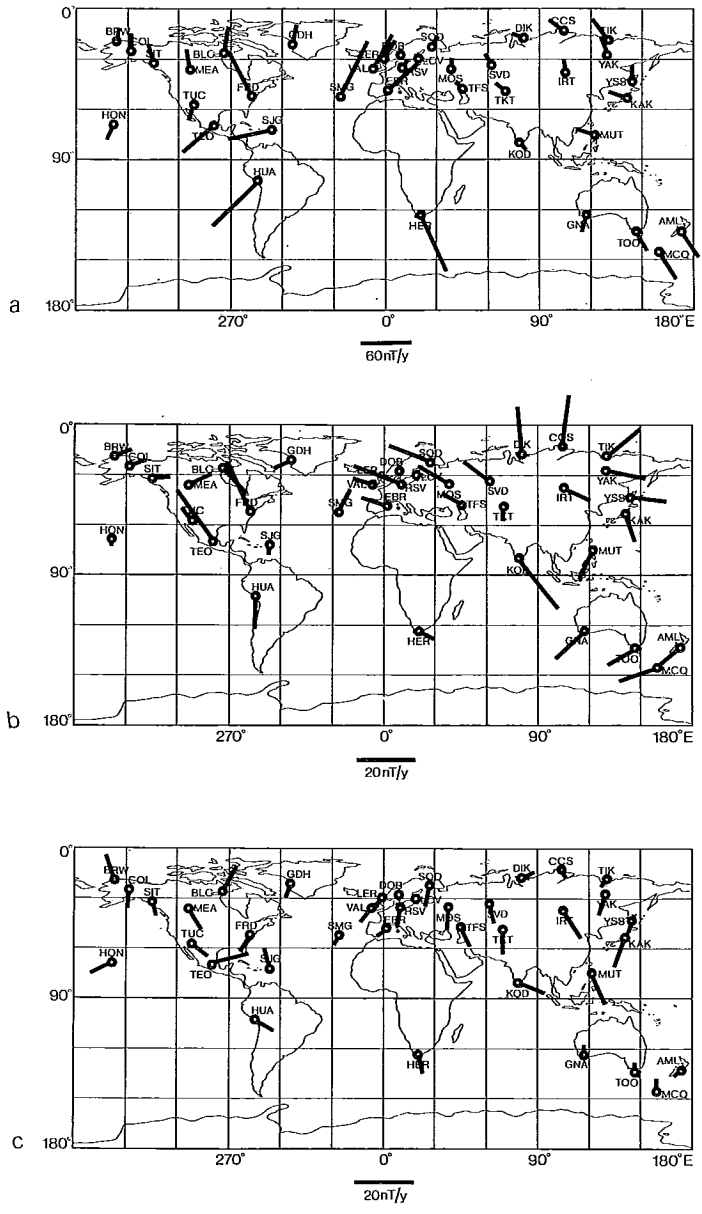

Fig. 8a. $(\dot{X}, \dot{Y})$ vectors of constant secular variation during 1953–75.
b. $(\dot{X}, \dot{Y})$ vectors of the 22-year wave for 1972.0.
c. Resultant of $(\dot{X}, \dot{Y})$ vectors of Fourier waves with periods of $2.2 \leqslant T \leqslant 11$ y, ($k = 2, 3, \ldots,$ 10) for 1972.0.

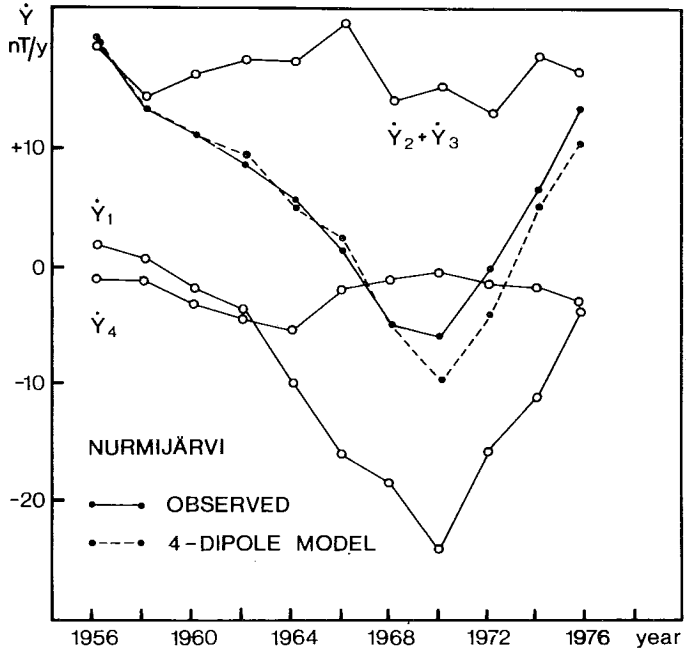

Fig. 9. The observed secular variation of Y (line with solid circles) at the Nurmijärvi observatory, Finland. The dotted curve depicts $\dot{Y}$ as calculated from the four-dipole model in Table 3. The curve denoted by $\dot{Y}_1$ represents the contribution of the dipole j = 1 describing the secular variation in Asia. The curve denoted by $\dot{Y}_2 + \dot{Y}_3$ represents the contribution of the dipoles j = 2 and 3 describing the secular variation of the Atlantic cell. $\dot{Y}_4$ represents the contribution from the dipole j = 4.

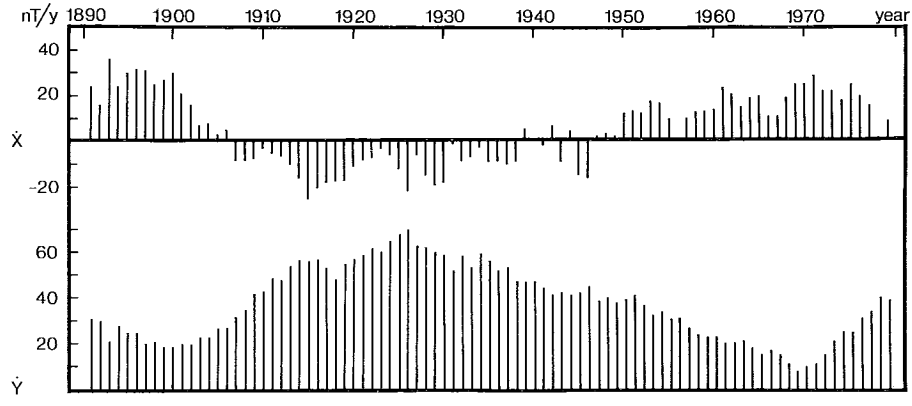

Fig. 10. Secular variation of X and Y at Niemegk observatory, GDR, and its predecessors Seddin and Potsdam.

In general, the directions of horizontal vectors $(\dot{X}, \dot{Y})$ around a $\dot{Z}$ focus $(\dot{Z}_f)$ are towards the focus if $\dot{Z}_f > 0$, and away from it if $\dot{Z}_f < 0$. As can be seen from Fig. 8b, the distribution of $(\dot{X}, \dot{Y})$ vectors for $T = 22$ y in Europe and Asia indicates a negative $\dot{Z}$ focus in Central Asia in agreement with $\dot{Z}$ charts in Figs. 1 and 2 based on the four-dipole model. The positive $\dot{Z}$ cell near the Antarctic (see Fig. 1 and 2) is also revealed by the vectors for the Australian observatories.

Globally, the Asian negative $\dot{Z}$ cell is dominating the secular variation of 22-year period. On the other hand, the main contributor to the constant part of the secular variation is the large negative $\dot{Z}$ cell in the Atlantic, as can be seen from Fig. 8a describing the constant part of $(\dot{X}, \dot{Y})$ vectors. Europe seems to belong to the boundary region of these two cells: in south-western Europe constant horizontal secular variation is dominant whereas in northern and eastern Europe the cyclic part is dominant (see also Fig. 9).

The cyclic secular variation after 1956 may be part of the so-called »60-year cycle» of the geomagnetic field (JIN and THOMAS [21], YUKUTAKE [38]). The secular variation in Europe around 1910 was very similar to that currently prevailing, as can be seen from recordings from Niemegk (GDR) (see Fig. 10), which is a typical Central European observatory. Fig. 11 shows that in Central Europe a high $\dot{Y}$ ($\gtrsim$40nT/y) corresponds to negative $\dot{X}$ values, $\ddot{Y} > 0$ implies $\ddot{X} < 0$, and vice versa.

The vectors describing the contributions of 11 to 2.2 year waves (Fig. 8c) have a roughly uniform global distribution, indicating that they are of mainly external origin caused by the magnetospheric ring current modulated by the 11-year solar activity cycle.

3.4 Global features of secular variation as revealed by SH dipole and quadrupole terms

Figs. 1 and 2 show that the secular variation of Z consists of one negative and two positive zones circling the Earth. The positive zones are located around the north and south poles, north of 50–60°N and south of 45°S. Between them is the negative zone. This distribution of $\dot{Z}$ corresponds to an SH axial quadrupole $(\dot{g}_2^0)$, which is thus the dominant term in the SH representation of secular variation (see Fig. 11). The axial dipole $(\dot{g}_1^0)$, if $\dot{g}_1^0 > 0$ and $\dot{g}_2^0 < 0$, distorts the quadrupole field so that the southern $\dot{Z}$ zone is larger and more intense than the southern one, as can be seen in Figs. 1 and 2.

The charts in Figs. 1 and 2 show that the absolute intensities of the Atlantic, Antarctic and Icelandic $\dot{Z}$ foci grew rapidly up to about 1970, after which their

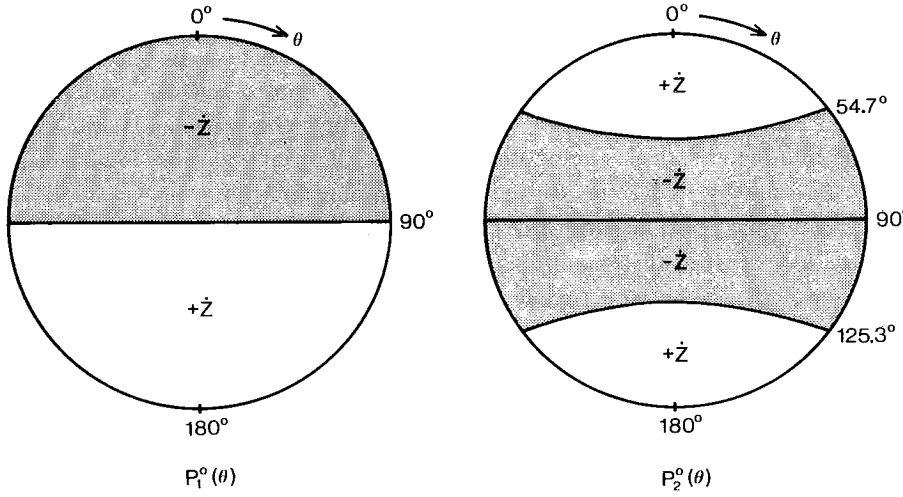

Fig. 11. Zones of positive and negative $\dot{Z}$ of the SH axial dipole (g_1^0) and quadrupole (g_2^0) fields when $\dot{g}_1^0 > 0$ and $\dot{g}_2^0 < 0$.

yearly rate has become slower. Globally the secular variation has been such that $\dot{Z}$ has become more negative in the northern hemisphere and more positive in the southern. In the SH representation this tendency means that $\dot{g}_1^0$ has increased, so the decrease in g_1^0 has accelerated. Using the method presented in chp. 2.1, which converts the parameters of the four-dipole model to SH coefficients, it can be shown that $\dot{g}_1^0$ has increased over twofold, from 10nT/y to 22nT/y, from 1956 to 1972 (see Fig. 5). The long-term average of $\dot{g}_1^0$ is 15nT/y (NAGATA [28]). The intensification of the $\dot{Z}$ focus near Iceland (see Figs. 1 and 2) reduces the $\dot{g}_1^0$ term but increases the absolute value of the quadrupole term $\dot{g}_2^0$, which has increased about 10 % during the time interval studied. The decrease of $\dot{g}_2^0$ intensifies and expands the equatorial zone of negative $\dot{Z}$. A consequence of this intensification is the northward drift of isoporic foci in the Atlantic shown in Fig. 3.

Since about 1970, the decrease of the strength of the axial dipole has weakened and the rate of the decrease in the strength of the axial dipole g_1^0 can be predicted to be slower in the near future.

4. *Conclusions*

A model of four changing radial dipoles at a distance of 0.25 R_e from the geocentre was applied to the observed global secular variation. was studied. The number of dipoles was limited to four partly because there are four main foci in the anomaly field and partly because the rather complicated computer program needed

for the minimization could not in reasonable time handle more complicated dipole models. The four-dipole model is shown to describe the global secular variation from 1956 to 1976 with a mean vector rms error of 8.9nT/y, which corresponds in accuracy to a 5th degree SH expansion. The four-dipole model consists of 24 coefficients, whereas the 5th degree SH model has 35 coefficients. The low number of coefficients in the four-dipole model may be due to the fact that eccentric dipoles better take into account the regional character of the isoporic field than does the SH expansion. The fact that only four dipoles are enough to obtain the rather low rms error means that a small number of discrete sources affect the global secular variation. However, the description of the anomaly field by the four-dipole model is not unique, because only secular variation data have been used to determine the dipole parameters. Thus the parameters can be used to calculate secular variation, but their connection with the anomaly field is obscure.

The isoporic field obtained by the dipole model shows that global secular variation accelerated from 1956 to 1970, and that the rate is now slightly slower. For example, $\dot{g}_1^0$ derived from the four-dipole model increased over 50 % from its long-term average of 15nT/y. The most dramatic change of the isoporic field occurred in Eurasia, where the Caspian $\dot{Z}$ cell drifted rapidly to the northeast and changed its sign from positive to negative. The present trend in Eurasia is towards positive $\dot{Z}$ values. The recent variations in the geomagnetic field have been quasi-cyclic with a period of about 20 years, but they might be a subharmonic of the 60-year cycle of the global geomagnetic field. As pointed out by COURTILLOT *et al.* [12], a rapid acceleration of secular variation seems to be connected with the variation in the Earth's rotation rate, indicating that these two phenomena are connected with each other.

Acknowledgements: This study was financially supported by Suomen Tiedeseura seuran Sohlbergin Delegaatio and Leo ja Regina Wainsteinin Säätiö.

REFERENCES

1. ALLDREDGE, L.R. and L. HURWITZ, 1964: Radial dipoles as the sources of the Earth's main magnetic field. *J. Geophys. Res.*, 69, 2631–2640.
2. –»– and C.O. STEARNS, 1969: Source of Earth's magnetic field and its secular change. *Ibid.*, 74, 6853–6593.
3. BARRACLOUGH. D.R., 1971: Secular variation in Scandinavia, *Nature*, 233, 94–98.
4. –»–, 1972: Geomagnetic secular variation in Scandinavia, *Ibid.*, 236, 96.
5. –»–, HARWOOD, J.M., LEATON, B.R. and S.R.C. MALIN, 1975: A model of the geomagnetic field at the epoch 1975. *Geophys. Res. J.R. astr. Soc.*, 43, 645–659.
6. –»–, HARWOOD, J.M., LEATON, B.R. and S.R.C. MALIN, 1978: A definitive model of the geomagnetic field and its secular variation for 1965 – I. Derivation of model and comparison with the IGRF. *Ibid.*, 55, 111–121.

7. BERGER, S. and A. BREKKE, 1978: Comparison of annual variations observed in the Earth's magnetic field at Tromsö, Ny-Aalesund and Bjørnøya. *Institute of Mathematical and Physical Sciences, Univ. of Tromsö.*
8. BOCHEV, A., 1978: Secular change of the Earth's magnetic field determined by the tridipole model of the main field for 1942–50. *C.R. Acad. Sci. Bulg.*, **31**, 297–300.
9. CAIN, J.C., 1979: Main field and its secular variation. *Rev. Geophys. Space Phys.*, **17**, 273–277.
10. –»– and S. HENDRICS, 1967: The geomagnetic secular variation, 1900–1965. Greenbelt, Md.,: *Goddard Space Flight Center.*
11. CHAPMAN, S. and J. BARTELS, 1940: *Geomagnetism I.* Oxford, Univ. Press.
12. COURTILLOT, V., DUCRUIX, J. and J.-L. LeMOUËL, 1978: Sur une accélération de la variation seculaire du champ magnétique terrestre. *C.R. Acad. Sci. Paris*, **287**, 1095–1098.
13. DAWSON, E. and L.R. NEWITT, 1978: An analytical representation of the geomagnetic field in Canada for 1975. Part II: The secular variation. *Can. J. Earth Sci.*, **15**, 237–244.
14. DOLGINOV, Sh.Sh., IVCHENKO, M.P., ORLOV, V.P., PUSHKOV, A.N., TYURMINA, L.O. and T.N. CHEREVKO, 1972: Secular geomagnetic field variations of the epoch 1965–70 according to observatory and satellite observations. *Geomagn. Aeron.*, **12**, 445–452.
15. FISHER, M.P., 1976: Annual means of geomagnetic elements since 1941. *Natural Environment Research Council, Inst. of Geol. Sci., Geomagn. Bull.*, 6.
16. HARWOOD, J.M. and S.R.C. MALIN, 1976: Present trends in the Earth's magnetic field. *Nature*, **259**, 469–471.
17. HURWITZ, L., 1960: Eccentric dipoles and spherical harmonic analysis. *J. Geophys. Res.*, **65**, 2555–2556.
18. –»–, KNAPP, D.G, FABIANO, E.B. and N.W. PEDDIE, 1973: Geomagnetic secular change, 1964–1970, from satellite F and observatory X, Y and Z. *Ibid.*, **78**, 8351–8255.
19. –»–, FABIANO, E.B. and N.W. PEDDIE, 1974: A model of the geomagnetic field for 1970.0. *Ibid.*, **79**, 1716–1717.
20. JAMES, F. and M. ROOS, 1975: MINUIT – A system for function minimization adn analysis of the parameter errors and correlations. *Comp. J. Comm.*, **10**, 343–367.
21. JIN, R. and D.M. THOMAS, 1977: Spectral line similarity in the geomagnetic dipole field variations and length of day fluctuations. *J. Geophys. Res.*, **82**, 828–834.
22. LANGEL, R.A., FABIANO, E.B. and G.D. MEAD, 1978: The utility of surface magnetic field measurements in the MAGSAT program. *NASA Technical Memorandum* No. 79614.
23. LEATON, B.R., 1962: Geomagnetic secular variation for the epoch 1955. *R. Obs. Bull.*, **57**, 245–270.
24. LOWES, F.J., 1955: Secular variation in the non-dipole field. *Ann. Geophys.*, **11**, 91–94.
25. –»– and S.K. RUNCORN, 1951: The analysis of the geomagnetic secular variation. *Phil. Trans. R. Soc. London*, Ser. A, **243**, 525–546.
26. MALIN, S.R.C., 1969: Geomagnetic secular variation and its changes, 1942.5 to 1962.5. *Geophys. J. R. astr. Soc.*, **17**, 415–441.
27. –»– and A.D. CLARK, 1974: Geomagnetic secular variation, 1962.5 to 1967.5. *Ibid.*, **36**, 11–20.

28. NAGATA, T., 1965: Main characteristics of recent geomagnetic secular variation. *J. Geomagn. Geoelectr.*, **17**, 263–276.
29. NEVANLINNA, H., 1979: The geomagnetic field and its secular variation in Finland and nearby countries. *J. Geophys.*, **46**, 201–216.
30. –»–, 1980: Interpreting regional geomagnetic anomalies and their secular change with the aid of radial dipoles and current loops. *J. Geomagn. Geoelectr.*, **32**, 13–36.
31. –»– and C. SUCKSDORFF, 1980: Comparisons of secular variation of two-dipole and spherical harmonic models with observatory data in Eurasia, 1965–75. *Proceedings of the 75th anniversary of the Ebro geomagnetic observatory*, (in press).
32. ORLOV, V.P., 1965: The leading trends of the secular variation investigations. *J. Geomagn. Geoelectr.*, **17**, 277–286.
33. PEDDIE, N.W., 1979: Current loop models of the Earth's magnetic field. *J. Geophys. Res.*, **84**, 4517–4523.
34. –»– and E.B. FABIANO, 1976: A model of the geomagnetic field for 1975. *Ibid.*, **81**, 2539–2542.
35. POCHTAREV, V.I., 1978: Dynamics of the Caspian center of secular geomagnetic field variations. *Geomagn. Aeron.*, **18**, 126–127.
36. PUSHKOV, A.N. and M.P. IVCHENKO, 1979: The summary of the annual mean values of magnetic elements at the world magnetic observatories. Vol. 14, *IZMIRAN, Acad. of Sci. of the USSR.*
37. TAZIMA, M., MIZUNO, H. and M. TANAKA, 1976: Geomagnetic secular change anomaly in Japan. *J. Geomagn. Geoelectr.*, **28**, 69–84.
38. YUKUTAKE, T., 1973: Fluctuations in the Earth's rate of rotation related to changes in the geomagnetic dipole field. *Ibid.*, **25**, 195–212.
39. –»– and H. TACHINAKA, 1968: The non-dipole part of the Earth's magnetic field. *Bull. Earthq. Res. Inst.*, **46**, 1027–1074.
40. –»– and H. TACHINAKA, 1969: Separation of the Earth's magnetic field into drifting and the standing parts. *Ibid.*, **47**, 65–98.
41. ZIDAROV, D., 1969: Geomagnetic field variations. *Geomagn. Aeron.*, **9**, 856–861.
42. –»– and A. BOCHEV, 1969: Representation of secular geomagnetic field variations as variations of the field of optimum geomagnetic dipoles. *Ibid.*, **9**, 252–256.
43. –»– and T. PETROVA, 1978: Representation of the Earth's magnetic field as a field of circular electric current loops. *C.R. Acad. Sci. Bulg.*, **31**, 663–666.